01 Jan 1971

An Approximate Model For The Static Operation Of A Fluidic Amplifier Employing Axisymmetric Jets

Richard T. Johnson
Missouri University of Science and Technology

Recommended Citation

R. T. Johnson, "An Approximate Model For The Static Operation Of A Fluidic Amplifier Employing Axisymmetric Jets," *Journal of Fluids Engineering, Transactions of the ASME*, vol. 93, no. 1, pp. 47 - 54, American Society of Mechanical Engineers, Jan 1971.
The definitive version is available at https://doi.org/10.1115/1.3425181

R. T. JOHNSON
Mechanical and Aerospace Engineering Department, University of Missouri, Rolla, Mo.
Assoc. Mem. ASME

An Approximate Model for the Static Operation of a Fluidic Amplifier Employing Axisymmetric Jets

An approximate mathematical model for the static, no-load (blocked receiver) operation of a fluidic amplifier employing axisymmetric jets is developed. The amplifier is similar in concept to the three-terminal modulator developed by the Johnson Service Co. The approach used in developing the model assumes that the complex flow phenomena can be represented by the combination of several elementary flow problems. The model employs the concept of an equivalent power nozzle in describing downstream flow with a control signal present. Experimental results are presented to justify assumptions and evaluate parameters.

Introduction

In the process of developing a novel fluidic device [1],[1] an approximate mathematical model for the behavior of two normally intersecting, axisymmetric jets impinging on a plane surface was developed. A schematic representation of the intersecting jets and impingement plane is given in Fig. 1. This configuration is similar in concept to the three-terminal modulator developed by the Johnson Service Co. [2].

Even though an approximate model for this type of jet interaction device was available [2], it was considered to be inadequate for the application being considered. The major problems with the existing model were:

1 It did not provide the type of information desired.
2 The range of application of the model was not appropriate to the geometry and flow ratios being considered.

Hence, a program to develop a mathematical model more suitable for the intended application was undertaken.

The complex nature of the flow fields produced by the jet interaction shown in Fig. 1 precluded a direct analysis. Keeping in mind that the basic objective was to develop a relationship between the receiver output pressure and the control jet pressure, it was assumed that the complex flow field could be described as a combination of several elementary cases that were more amenable to analysis. The problem was separated into four areas of study:

1 The elementary submerged jet
2 A submerged jet impinging normally on a plane
3 Downstream longitudinal velocity fields produced by the normal intersection of two axisymmetric jets
4 Pressure distribution on the receiver plane due to the altered velocity profiles produced by the jet intersection.

In the following sections each segment of the model is examined and analytical and experimental results are presented. The concluding sections combine the separate segments examined and demonstrate experimental correlations and discrepancies.

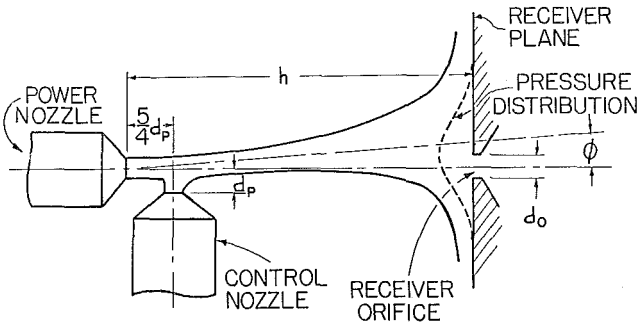

Fig. 1 Schematic diagram of intersecting jets impinging on a plane

[1] Numbers in brackets designate References at end of paper.

Contributed by the Fluidics Committee of The American Society of Mechanical Engineers and presented at the Joint Automatic Control Conference, Atlanta, Ga., June 22–26, 1970. Manuscript received at ASME Headquarters, April 2, 1970. Paper No. 70-Flcs-4.

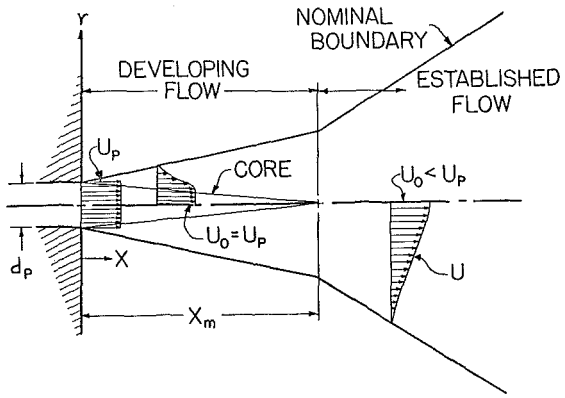

Fig. 2 Schematic diagram of two-region jet

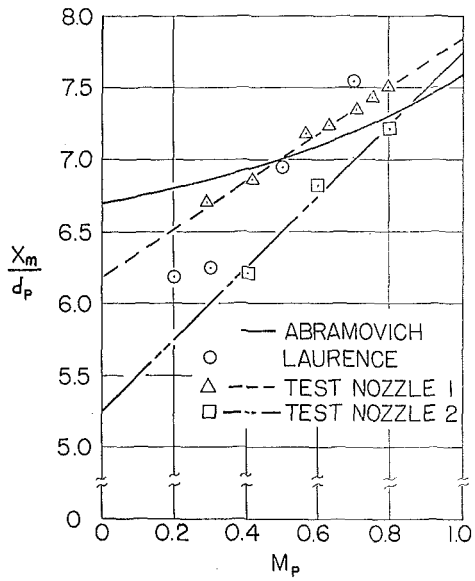

Fig. 3 Functional relation between apparent core length and exit Mach number

Elementary Submerged Jet

The submerged jet is a classic problem in the fluid mechanics and gas dynamics areas. Considerable work has been done in the study of incompressible turbulent jets and in the study of supersonic jets. The subsonic turbulent jet attracted relatively little interest until its use in fluidic devices demonstrated the need for information in this area.

An additional problem, posed by geometry requirements in fluidic devices, is describing the effect of nonstandard and unusual nozzle geometries on the turbulent jet. In order to denote the effects of nozzle geometry and slight compressibility on the submerged jet, a brief review of the ideal incompressible submerged jet is appropriate.

One of the classic studies of the incompressible jet was made by Albertson, et al. [3]. Fig. 2 is a schematic of the jet development pattern assumed in this study. The jet flow is divided into two regions: the developing flow region and the established flow region. In the developing flow region, turbulent mixing effects are present on the outer boundary of a potential flow core. When turbulent mixing is completed, the potential flow core has dissipated and the longitudinal velocity profile takes on a shape similar to that shown in Fig. 2. The nominal dividing line between the two flow regions is considered to be at the end of the potential core when $x = x_m$.

The description of longitudinal velocity fields in the established flow region was of primary interest in this study. Albertson, et al. [3] show that for the incompressible case

$$\frac{U}{U_p} = \left(\frac{d_p}{2Cx}\right) \exp\left(-\frac{r^2}{2C^2x^2}\right) \tag{1}$$

where $x > x_m$ and C is a constant used to describe the relative width of the velocity distribution. For a given incompressible jet the value of C is fixed.

In order to extend this type of velocity field description to the slightly compressible flow cases of interest, several assumptions were necessary. They were:

1 Temperature gradients in the jet are small enough to allow heat transfer effects to be negligible.

Nomenclature

A_o = effective area of output orifice
A_p = relative width of pressure distribution in receiver plane
A_v = relative width of velocity profile in established flow region
B_p = lateral displacement of center of pressure distribution
B_{pc} = uncorrected lateral displacement of center of pressure distribution
B_v = lateral displacement of center of velocity profile at some arbitrary station in the established flow region
C = constant used in the development of an analytical model for an incompressible, turbulent jet
d_0 = diameter of output orifice
d_p = power nozzle diameter
E,F = constants used to descibe the variation of the inviscid core length, x_m, in terms of the exit Mach number, $\mathbf{M}_p$
g_c = gravitational constant
h = nozzle-to-plane distance
k_1 = constant used to adjust gas density
$\dot{m}_c$ = mass flow rate from control jet
$\dot{m}_p$ = mass flow rate from power jet
$\mathbf{M}_p$ = Mach number at power jet exit
P_{amb} = ambient pressure
P_{av} = average output pressure
P_C = control jet stagnation pressure
P_D = change in P_{av} from some bias level
P_E = power jet stagnation pressure
P_0 = stagnation pressure at point 0 on plane
P_{oc} = computed output pressure
P_s = pressure at any point on receiver plane
P_{sm} = maximum pressure on receiver plane
R = specific gas constant
r = radial distance from centerline of undisturbed power jet
r_o = effective radius of output orifice
T_p = power jet stagnation temperature
T_1 = static temperature at point 1
U = longitudinal velocity at any point in jet field
U_c = control jet exit velocity
U_0 = centerline velocity of jet at any longitudinal location
U_p = power jet exit velocity
U_1 = centerline velocity of jet at point 1
V_s = acoustic velocity at power jet exit
x = longitudinal distance from power jet exit
x_m = length of inviscid core
α = parameter related to inviscid core length
β = parameter used in the development of a model for the pressure distribution on the receiver plane
ϕ = angular rotation of jet centerline
ρ_1 = gas density at point 1
$'$ = indicates that symbol used is associated with the effective jet

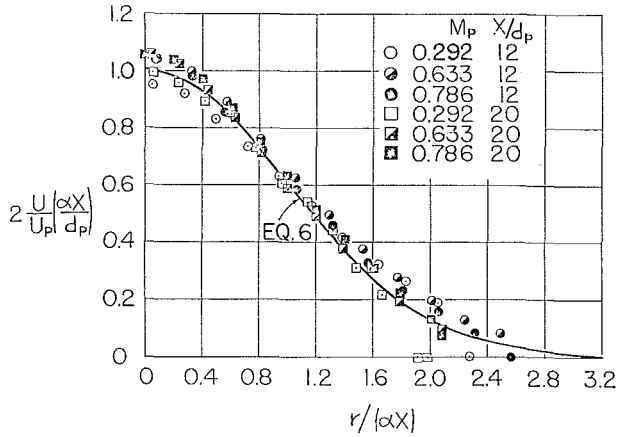

Fig. 4 Nondimensional longitudinal velocity distribution in the region of established flow

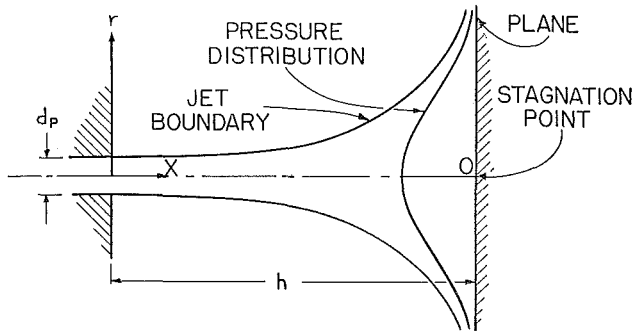

Fig. 5 Schematic diagram of jet impinging on a normal plane

2 Static pressure in the jet is essentially ambient pressure.

3 Basic jet structure is unchanged.

4 Nozzle exit velocity is low enough to preclude the presence of shock phenomena.

Based on these assumptions, a relatively simple way to account for compressibility and nozzle geometry effects was to allow the constant C to be a parameter which varies with nozzle exit Mach number, $\mathbf{M}_p$. This is equivalent to letting

$$x_m = f(\mathbf{M}_p) \tag{2}$$

Since x_m is a simple function of C, the parameter α was used to replace C and

$$\alpha = \frac{d_p}{2x_m} \tag{3}$$

Abramovich [4] and Laurence [5] have also published work that employs this concept of a nozzle parameter sensitive to exit Mach number. Fig. 3 presents their findings plus experimental data for two nozzles used in this investigation. The curve from Abramovich is based on an analytical development and the remaining data are experimental in nature. Since the experimental data were readily described using straight lines, the general form for the functional relation expressed in equation (2) was assumed as

$$\frac{x_m}{d_p} = E(\mathbf{M}_p) + F \tag{4}$$

where E and F are constants dependent upon the nozzle geometry. Combining equations (3) and (4) yields

$$\alpha = \frac{1}{2[E(\mathbf{M}_p) + F]} \tag{5}$$

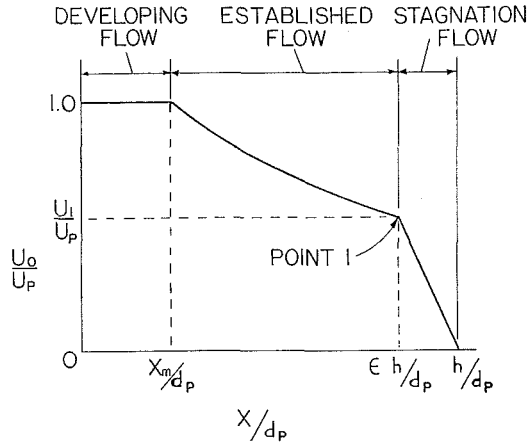

Fig. 6 Assumed centerline velocity decay of the impinging jet

Substitution of α for C in equation (1) and a slight rearrangement of terms yields the following nondimensional equation for the longitudinal velocity fields in the established flow region:

$$2\frac{U}{U_p}\left(\frac{\alpha x}{d_p}\right) = \exp\left[-\left(\frac{r}{\sqrt{2}\,\alpha x}\right)^2\right] \tag{6}$$

The validity of this equation in the range $0.292 \leq \mathbf{M}_p \leq 0.786$ and $12 \leq x/d_p \leq 20$ is illustrated by the good correspondence with experimental evidence shown in Fig. 4.

Submerged Jet Impinging Normally on a Plane

The intent of this portion of the investigation was to describe the pressure distribution on a plane produced by a submerged jet impinging normally upon it. To be of significant value the description was to employ only the exit conditions of the jet, the jet nozzle-to-plane geometry, and any necessary experimental constants or parameters. The geometry and nomenclature for the impinging jet are shown in Fig. 5.

Potential flow theory was used by Rouse [6] and Schlichting [7] to describe the flow in the vicinity of the stagnation point for impinging flow situations similar to this one. Their methods are used in reference [8] to develop the following equation for the pressure distribution on the plane in the vicinity of the stagnation point:

$$\frac{P_s}{P_0} = 1 - \beta^2\left(\frac{r}{h}\right)^2 \tag{7}$$

where P_s is the pressure at any point, P_0 is the stagnation pressure at point 0, and β is an experimentally determined parameter.

The work of Banks and Chandrasekhara [9] and Poreh and Cermak [10] indicated that the actual pressure distribution on the plane was satisfactorily described by an equation of the form

$$\frac{P_s}{P_0} = \exp\left[-\beta^2\left(\frac{r}{h}\right)^2\right] \tag{8}$$

To compare this model with that obtained from potential flow theory, the right side of equation (8) was expanded in series form.

$$\exp\left[-\beta^2\left(\frac{r}{h}\right)^2\right] = 1 - \beta^2\left(\frac{r}{h}\right)^2 + \frac{\beta^4}{2!}\left(\frac{r}{h}\right)^4 - \ldots \tag{9}$$

Equation (9) indicates that the potential flow model of equation (7) and the empirical model of equation (8) are comparable for small values of r/h in the vicinity of the stagnation point.

In order to relate this description of the pressure distribution to the exit conditions of the jet, the stagnation pressure P_0 must be written in terms of the upstream characteristics. Since point 0 is on the jet centerline, the most obvious approach is to try to write P_0 in terms of the centerline velocity. Fig. 6 shows the

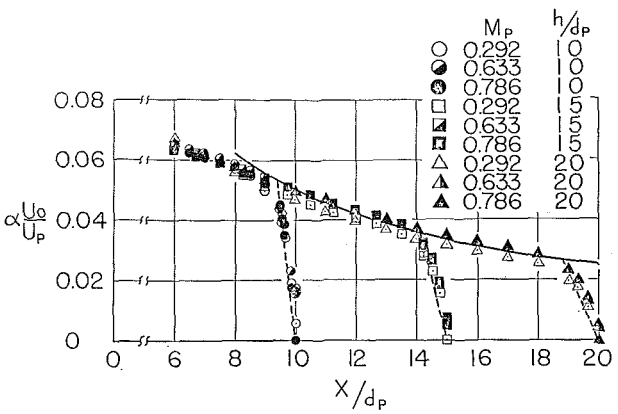

Fig. 7 Actual centerline velocity decay of the impinging jet

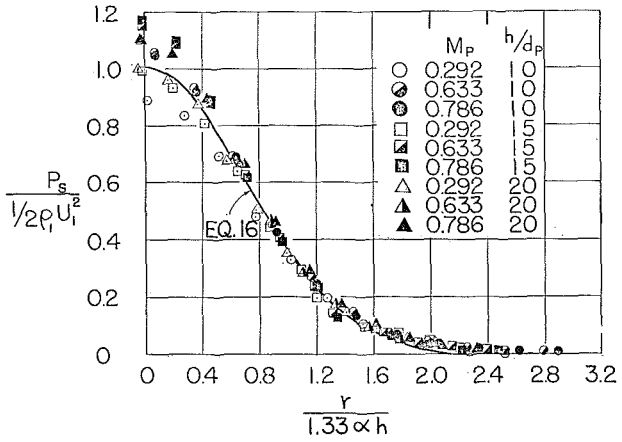

Fig. 8 Pressure distribution on plane due to impinging jet

combination of the centerline velocity for the free jet and the centerline velocity in the vicinity of the plane developed from potential flow theory in reference [8]. At point 1, where $x/d_p = \epsilon\, h/d_p$, the presence of the plane is first reflected in the value of the centerline velocity. Considering the flow incompressible, it is logical to assume that the stagnation process begins at this point and that the stagnation pressure, P_0, may be expressed as

$$P_0 = \tfrac{1}{2}\rho_1 U_1^2 \tag{10}$$

where U_1 and ρ_1 are, respectively, the velocity and density at point 1. Fig. 7 and equation (11), which was developed in reference [8] using the information shown in Fig. 7, substantially verify the assumptions leading to equation (10). The potential theory development for the equation describing the centerline velocity in the vicinity of the stagnation point is presented in reference [8]. The final result, verified by the data shown in Fig 7, was

$$\alpha \frac{U_0}{U_p} = \frac{8.65}{h/d_p}\left(1 - \frac{x}{h}\right) \tag{11}$$

for

$$0.94h/d_p < x/d_p < h/d_p$$

The empirical constant, 8.65, represented values of β ranging from 10.1 to 11.3 for the exit conditions examined. These values compare favorably with the value of $\beta = 11.18$ established by Banks and Chandrasekhara [9].

In order to use equation (10), values for ρ_1 and U_1 must be determined. The equation for the centerline velocity decay in the free jet is

$$\frac{U_0}{U_p} = \frac{d_p}{2\alpha x} \tag{12}$$

For point 1, $x = 0.94h$. Hence

$$U_1 = \frac{U_p d_p}{1.88\alpha h} \tag{13}$$

To simplify the computation of ρ_1, two assumptions can be made. The first assumption is that the ideal gas equation of state is valid at point 1. The second assumption is that the static pressure throughout the free jet is essentially ambient. The static temperature at point 1 has a fairly important effect on the density calculation. This is unfortunate since an accurate description of the temperature at this point is very difficult to obtain. The approximate relation

$$\frac{T_1}{T_p} = \exp\left[-\left(3.5\,\frac{M_p}{h/d_p}\right)^2\right] \qquad 0.015 \leq \frac{M_p}{h/d_p} \leq 0.08 \tag{14}$$

was developed from static temperatures that were computed considering measured stagnation pressures to be due to isentropic compression. In this equation T_1 is the static temperature at point 1 and T_p is the stagnation temperature at the jet exit.

Combining the above assumptions and approximate temperature relationship, the approximate density at point 1 can be computed using the following relationship:

$$\rho_1 = \frac{P_{amb}}{Rg_c T_p \exp\left[-\left(3.5\,\frac{M_p}{h/d_p}\right)^2\right]} \tag{15}$$

where P_{amb} is the ambient pressure, T_p is the jet exit stagnation temperature, and R and g_c are the gas and gravitational constants.

To complete the description of the free jet impinging on a plane, one more relationship is necessary. That relationship is one between the shape of the longitudinal velocity field of the free jet and the shape of the pressure distribution on the plane. Equations (6) and (8) indicate that the two distributions are both described by an exponential distribution involving r^2. The obvious assumption of a simple stagnation of the entire velocity distribution proves to be invalid. The changing direction of flow in the vicinity of the plane produces a spreading effect on the jet. A convenient assumption that appears to account for this effect is that the relative width of the pressure distribution is equal to that of the velocity distribution at point 1 where $x = 0.94h$. This assumption yields

$$\frac{P_s}{\frac{1}{2}\rho_1 U_1^2} = \exp\left[-\left(\frac{r}{1.33\alpha h}\right)^2\right] \tag{16}$$

The relative width of these distributions is

$$A_v = A_p = 1.33\alpha = \sqrt{2}(0.94)\alpha \tag{17}$$

where A_v is the relative width of the velocity distribution and A_p is the relative width of the pressure distribution.

The validity of these assumptions is demonstrated in Fig. 8 which shows the correlation of equation (16) with experimental data. Equations (14–17) represent the desired description of the pressure distribution on the plane in terms of the jet exit conditions and the nozzle-to-plane geometry.

Downstream Longitudinal Velocity Fields Produced by the Normal Intersection of Two Axisymmetric Jets

The preceding section demonstrated that the pressure distribution on a plane due to a normally impinging jet was directly related to the downstream longitudinal velocity field at 94 percent of the nozzle-to-plane distance. This section deals with the description of this velocity field under the influence of a control jet located at right angles to the main or power jet. Fig. 9 is a schematic diagram showing the orientation of the jets.

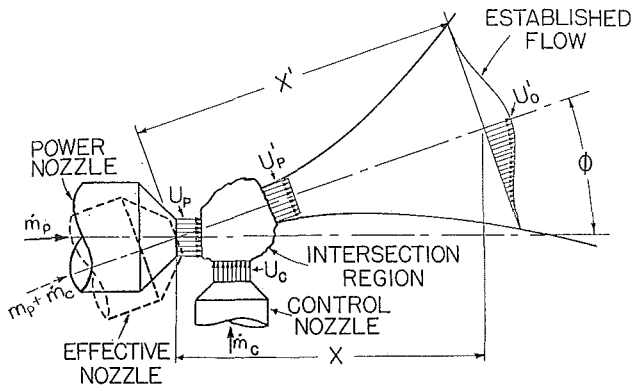

Fig. 9 Schematic of intersecting jets

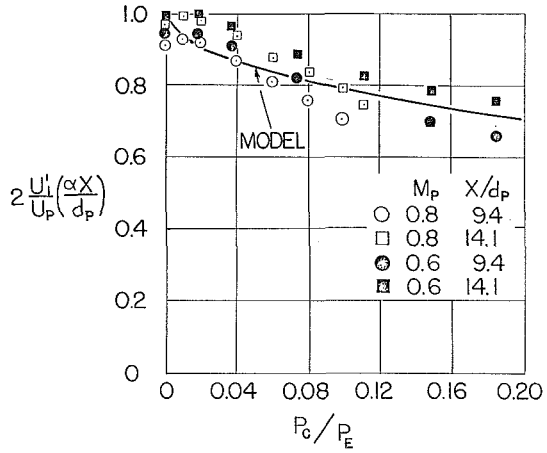

Fig. 10 Maximum velocity of effective jet in established flow region

Many authors have examined the problem of intersecting jets. Most investigations have concerned planar jets confined between parallel plates and the results are not directly applicable to this study. Lechner and Wambsganss [2] report on a device which employs axisymmetric jets intersecting at right angles. Although they did not investigate the velocity fields produced by the phenomenon, they obtained experimental evidence to validate the two following assumptions:

1 The pressure in the interaction region of the two jets could be considered to be atmospheric.

2 The two jet streams definitely merged into one stream containing the masses of the two original streams.

Camarata [11] and Olson [12] have discussed the concept of an "effective jet" to represent downstream characteristics with control flow. Both authors note and describe the alteration of inviscid core length and other jet characteristics. This "effective jet" concept was the basic approach used in this study.

In developing a mathematical description for the intersecting jet phenomena several additional assumptions were necessary. These were:

1 Linear momentum flux is conserved in the region of interaction and at all downstream locations.

2 The two jet nozzles are placed sufficiently close together so that their velocity fields are uniformly distributed upon entering the intersection region.

3 For the purposes of calculation, the flow leaving the intersection region can be considered to have a uniform velocity distribution.

4 At points sufficiently far downstream from the intersection region the flow field can be considered that of a free submerged jet with new exit conditions.

5 Downstream in the established flow region the flow will display an axially symmetric longitudinal velocity distribution which can be described by an exponential distribution of the Gaussian type. This distribution can be adequately described at any location by the following characteristics:

a A maximum value of velocity

b A number relating the width of the distribution to the maximum velocity

c A displacement of the axis of symmetry from the centerline of the original undisturbed free jet.

Referring to Fig. 9 and employing simple momentum exchange relations yields

$$U_p' = \frac{\sqrt{(\dot{m}_p U_p)^2 + (\dot{m}_c U_c)^2}}{\dot{m}_p + \dot{m}_c} \tag{18}$$

and

$$\tan \phi = \frac{\dot{m}_c U_c}{\dot{m}_p U_p} \tag{19}$$

where:

U_p' = effective nozzle exit velocity
U_p = actual power nozzle exit velocity
U_c = control nozzle exit velocity
$\dot{m}_p$ = mass flow rate through power nozzle
$\dot{m}_c$ = mass flow rate through control nozzle
ϕ = angular deflection of effective jet

Using equation (5) and the Mach number of the effective jet, $\mathbf{M}_p' = U_p'/V_s$, the inviscid core length parameter, α', of the effective jet is found to be:

$$\alpha' = \frac{d_p'}{2d_p(E\mathbf{M}_p' + F)} \tag{20}$$

where:

d_p = power nozzle diameter
$\mathbf{M}_p'$ = Mach number of effective jet
V_s = acoustic velocity at power nozzle exit conditions
d_p' = diameter of effective jet nozzle found from continuity considerations

By letting $r = 0$ in equation (6), and considering the geometry shown in Fig. 9, the following equation for centerline velocities can be developed:

$$2\left(\frac{U_0'}{U_p}\frac{\alpha x}{d_p}\right) = \left(\frac{U_p'}{U_p}\right)\left(\frac{\alpha d_p'}{\alpha' d_p}\right)\cos\phi \tag{21}$$

U_0' is the velocity at any point on the centerline of the effective jet in the established flow region. Note that this equation describes a downstream velocity in terms of the exit conditions of the effective and undisturbed jets.

The equation for any longitudinal velocity of the effective jet in the established flow region is obtained by using effective jet parameters in equation (6). Hence

$$2\left(\frac{U'}{U_p}\frac{\alpha x}{d_p}\right) = \exp\left[-\left(\frac{r'}{\sqrt{2}\,\alpha' x'}\right)^2\right] \tag{22}$$

where r' is a radial distance measured from the effective jet centerline and x' is a distance measured along the centerline. It is worthwhile to note that for most practical situations the angle ϕ is quite small and $\cos\phi \doteq 1$. For this case r' and x' in equation (22) can be replaced by r and x with no significant effect.

Examination of equation (22) shows that the relative width of the effective jet, A_v', can be expressed as:

$$A_v' = \sqrt{2}\alpha' \tag{23}$$

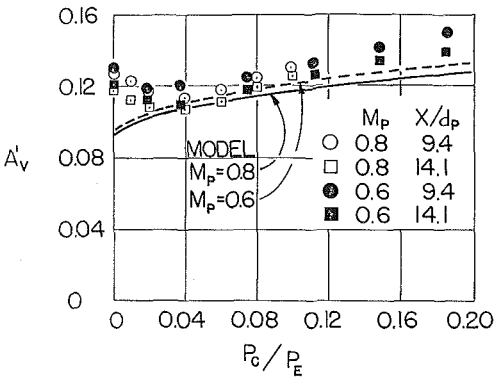

Fig. 11 Relative width, A_v', of effective jet in established flow region

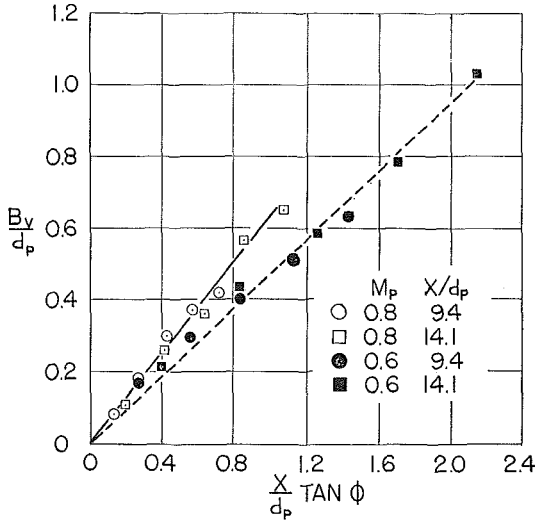

Fig. 12 Angular deflection of effective jet—experimental correlation

Descriptions for the maximum velocity and relative width of the effective jet have been developed. Their correspondence with experimental measurements is illustrated in Figs. 10 and 11. The independent variable is taken as the ratio of control jet stagnation pressure, P_C, to power nozzle stagnation pressure, P_E. This was considered appropriate since the output and input signals are usually defined in terms of pressures.

A description of the angular deflection of the effective jet was found to be more conveniently expressed in terms of the deflection of the jet centerline at an arbitrary downstream location in the established flow region. Designating this deflection at any location x as B_v, simple geometry yields:

$$\frac{B_v}{d_p} = \frac{x}{d_p} \tan \phi \tag{24}$$

This relationship assumes that the effective turning point for the jet is at the exit of the undisturbed jet. In reference [8] this assumption is verified for the geometry and pressure ratios considered in this study. Fig. 12 illustrates the correlation between experimentally measured values of B_v and those indicated by equation (24). By noting that the slope of the line shown is a function of the exit Mach number the following adjusted equation can be obtained:

$$\frac{B_v}{d_p} = 0.78 \frac{x}{d_p} M_p \tan \phi \tag{25}$$

where 0.78 is an experimental constant obtained from the data of Fig. 12.

The three quantities required to describe the downstream velocity fields have been expressed mathematically in equations (21), (23), and (25). Figs. 10, 11, and 12 illustrate the correlation between these equations and experimental evidence. In examining Figs. 10 and 11 a distinct discrepancy between the data and the model can be noted. This discrepancy is caused by the presence of the control nozzle in the vicinity of the undisturbed jet. Apparently the control nozzle introduces a drag force in the undisturbed jet which affects the downstream characteristics. As control flow is increased the drag effect is overcome and the jet begins to reestablish itself. The test configuration that produced these results was selected to provide a compromise between the control jet effect and the drag effect of the control nozzle. A more complete description of the geometry and test apparatus is given in reference [8].

Pressure Distribution on Receiver Plane Due to Effective Jet

In order to predict the output pressure of this fluidic "amplifier" a satisfactory description of the pressure distribution on the receiver plane was required. In particular, the description of the pressure distribution due to the effective jet was desired. The most direct approach to developing this description was to apply the information obtained in the study of the jet impinging normally on a plane. This jet was satisfactorily described by an exponential distribution with two parameters: a maximum value and a relative width. One additional parameter will be needed to describe the pressure distribution due to the effective jet. This parameter is the lateral displacement of the center of the distribution.

The maximum pressure of the distribution, P_{sm}, was initially assumed to be of the form

$$P_{sm} = \tfrac{1}{2}\rho_1 (U_1')^2 \tag{26}$$

where U_1' is the velocity on the centerline of the effective jet at $0.94h$. The following relation for U_1' may be developed using equation (13).

$$U_1' = \frac{U_p'}{1.88\alpha\, h/d_p} \tag{27}$$

Preliminary results indicated that the maximum pressure predicted by equation (26) was consistently too low. After some thought it was concluded that some adjustment of the density, ρ_1, was in order to bring the predicted values more in line with experimental results. The value of ρ used to compute P_{sm} was taken as

$$\rho \doteq \rho_1 \left(1 + \frac{k_1}{U}\right) \tag{28}$$

This relationship for ρ crudely accounts for the increase in density during stagnation. Since ρ is a function of U the stagnation pressure must be written:

$$P_{sm} \doteq \int_0^{U_1} \rho_1 \left(1 + \frac{k_1}{U}\right) U dU \doteq \rho_1 (\tfrac{1}{2}U_1^2 + k_1 U_1) \tag{29}$$

The experimental constant k_1 was found to be 35. The equation for computing P_{sm} was thus:

$$P_{sm} = \rho_1 (\tfrac{1}{2}U_1^2 + 35U_1) \tag{30}$$

For higher exit Mach numbers this equation tended to reduce some of the variations shown in Fig. 8. However, at very low exit Mach numbers the variations were more pronounced. Since these low Mach number conditions had been discarded as possible operating conditions, equation (30) was considered acceptable. Fig. 13 compares calculated and experimental results.

Using equations (30) and (16) the following equation was developed to describe the pressure about the center of the distribution:

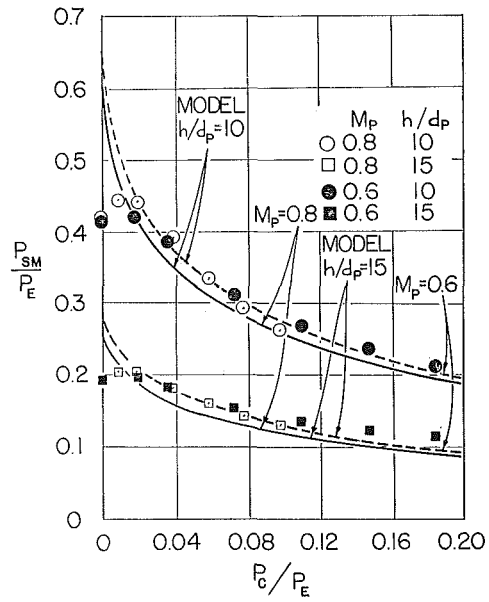

Fig. 13 Maximum pressure on plane due to effective jet

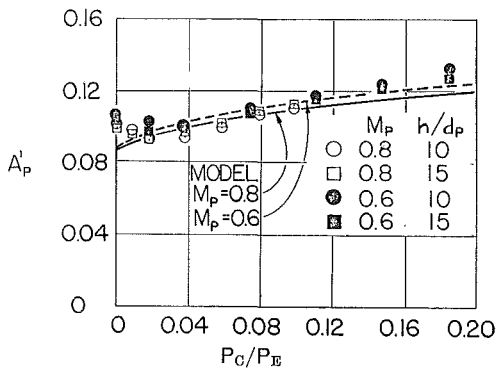

Fig. 14 Relative width, A_p', of pressure distribution due to effective jet

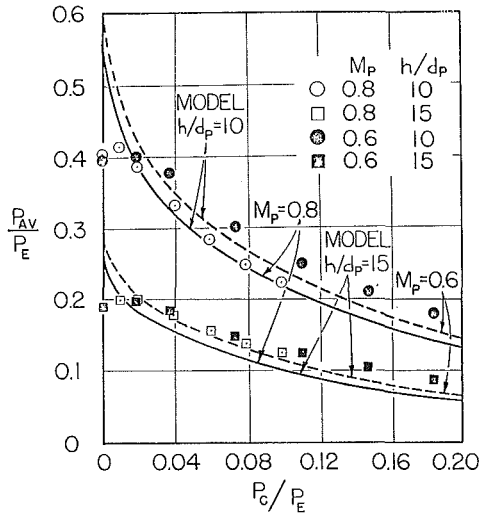

Fig. 15 Amplifier output pressure—blocked receiver

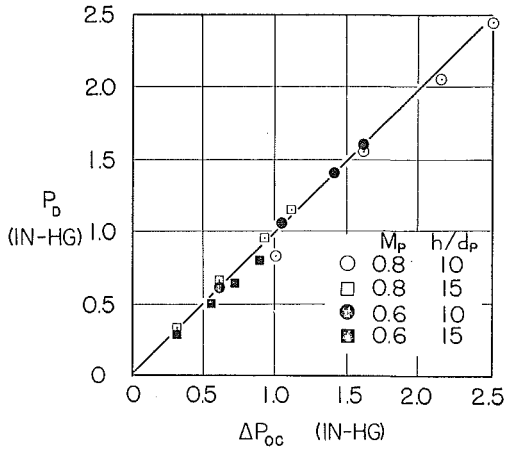

Fig. 16 Change in output pressure—measured versus computed

$$\frac{P_s}{P_{sm}} = \exp\left[-\left(\frac{r}{1.33\alpha' h}\right)^2\right] \tag{31}$$

The relative width term in the equation is

$$A_p' = 1.33\alpha'$$

Fig. 14 compares computed and experimentally determined values A_p'.

When equation (25) was used to describe the location of the center of the pressure distribution when $x = h$, several discrepancies were noted. The cause for this problem was assumed to be related to a momentum exchange problem when the jet impinges the plane at a slightly skew angle. An empirical correction was developed:

$$\frac{B_p}{d_p} = \left(0.028\,\frac{h}{\mathbf{M}_p d_p} + 0.32\right)(B_{pc})^{\left(0.0192\,\frac{h}{\mathbf{M}_p d_p} + 0.52\right)}$$

$$B_{pc} = 0.78\mathbf{M}_p\,\frac{h}{d_p}\tan\phi \tag{32}$$

$$12.5 \leq \frac{h}{\mathbf{M}_p d_p} \leq 25$$

B_p is the lateral deflection of the center of the pressure distribution on the plate and B_{pc} is the value computed from equation (25). A more thorough discussion of this problem and its analysis is included in reference [8].

Amplifier Output

The preceding section presented the analytical description of the pressure distribution on the receiver plane. To find the output pressure for a given receiver orifice it would seem logical simply to find the average pressure acting over the area of the orifice for any given control condition. This is, fundamentally, the approach that is used. However, because the dimensions of a reasonable output orifice are relatively large compared to the dimensions of the pressure distribution, pressure gradients exist across the output orifice. These gradients can be large enough to cause recirculating flow problems—especially in blocked receivers. In most cases this effect is reflected in behavior typical of a receiver of smaller area than actually exists. Hence, the concept of an "effective receiver diameter or width" has developed. Olson [12] examines this problem is somewhat more detail.

By removing the control nozzle assembly and observing the pressure produced by the impinging jet on the receiver, the effective receiver diameter was estimated to be 73 percent of the actual diameter. Using this value for a receiver diameter, the output pressure for various control pressures was computed. Comparison of computed and measured outputs is given in Fig. 15.

Since operation of an amplifier such as this one is usually considered in terms of the change in output about some bias, it was deemed worthwhile to examine the output about some bias. The bias level chosen was one large enough to avoid the region of operation where control nozzle drag seriously influences the behavior. Fig. 16 demonstrates that the model developed predicts the output characteristics of the blocked receiver amplifier for the range of interest. Equation (33) expresses the relation between the characteristics of the effective jet and the change in output pressure.

$$\Delta P_{oc} = \frac{\rho_1(\frac{1}{2}U_1'^2 + 35U_1')}{A_0} \times \int_0^{2\pi}\int_0^{0.73r_0} \exp\left[-\frac{(r^2 + B_p^2 - 2B_p r\cos\theta)}{2(\alpha')^2h^2}\right] rdrd\theta - \frac{\rho_{1b}(\frac{1}{2}U_{1b}'^2 + 35U_{1b}')}{A_0} \times \int_0^{2\pi}\int_0^{0.73r_0} \exp\left[-\frac{(r^2 + B_{pb}^2 - 2B_{pb}r\cos\theta)}{2(\alpha_b')^2h^2}\right] rdrd\theta \quad (33)$$

where U_1', α', B_p are properties of the effective jet and b subscripts denote the bias condition.

Conclusion

The model presented was not intended to be extremely general in nature. However, the agreement between the model and experimental results lends significant validity to this type of modeling approach. The results of this work indicate that the concept of studying a complicated flow problem by dividing it into simpler, more easily modeled parts, could develop into a useful analysis technique.

References

1 Johnson, R. T., and Trummel, J. M., "A Fluidic Transmitter," *Proceedings of the Joint Automatic Control Conference*, Boulder, Colo., Aug. 1969.

2 Lechner, T. J., and Wambsganss, M. W., "Proportional Power Stages for Impedance Matching Pure Fluid Devices," *Fluid Amplifier Symposium*, Diamond Ordnance Fuse Laboratories, Washington, D. C., Oct. 1962.

3 Albertson, M. L., Dai, Y. B., Jenson, R. A., and Rouse, H., "Diffusion of Submerged Jets," *Proceedings of the American Society of Civil Engineers*, Vol. 74, No. 10, Dec. 1948.

4 Abramovich, G. N., *The Theory of Turbulent Jets*, (translation from Russian) M.I.T. Press, Cambridge, Mass., 1963.

5 Laurence, J. D., *Intensity, Scale and Spectra of Turbulence in Mixing Region of Free Subsonic Jet*, N.A.C.A. Report 1292, 1956.

6 Rouse, H., ed., *Advanced Mechanics of Fluids*, John Wiley and Sons, New York, N. Y., 1959.

7 Schlichting, H., *Boundary Layer Theory*, 4th ed., McGraw-Hill, New York, 1960.

8 Johnson, R. T., "Fluid Jet Transmission of a Pressure Signal From a Rotating Shaft to a Fixed Receiver," PhD thesis, Department of Mechanical Engineering, University of Iowa, Feb. 1968.

9 Banks, R. B., and Chandrasekhara, D. V., *Hydromechanics of a High Velocity Gas Jet Penetrating a Liquid Surface*, Final Progress Report for the Bureau of Ships, Department of the Navy, prepared by the Technological Institute, Northwestern University, Evanston, Ill., and the Fluid Mechanics Research Laboratory, SEATO Graduate School of Engineering, Bangkok, Thailand, March, 1962.

10 Poreh, M., and Cermak, J. E., "Flow Characteristics of a Circular Submerged Jet Impinging Normally on a Smooth Boundary," Sixth Midwestern Conference on Fluid Mechanics, The University of Texas, 1959.

11 Camarata, T. J., "Analytical Procedure for Predicting Performance of Single-Stage Momentum Exchange Proportional Amplifiers," *Advances in Fluidics*, 1967 Fluidics Symposium, ASME, New York.

12 Olson, R. E., "Analytical Techniques for Predicting the Characteristics of Jet Flows in Fluid Devices," *Fluidics Quarterly*, Vol. 1, 1967.